STM JOURNALS

Journal of
Polymer & Composites

https://journals.stmjournals.com/jopc

ISSN: 2321-2810 (Online)
ISSN: 2321-8525 (Print)
Volume 14, Special Issue 2, 2026
DOI (Journal): 10.37591/JoPC

Research JoPC

Experimental Investigation and Optimization of Machining Parameters for Al6351 Alloy Using a Modified Taguchi Approach

Suthapalli Satya Surya Sai Lokesh[1]*, K. Sri Manikanta[2], Boggarapu Nageswara Rao[3], K. Prasanth Kumar Reddy[4], V. Sai Akshara[5], Muni Tanuja Anantha[6]

Abstract

Machining processes encompass both conventional and non-conventional techniques and optimizing machining parameters is crucial for achieving high-quality outcomes. However, simplifying these processes remains a significant challenge. This study focuses on determining the optimal machining parameters—cutting speed, feed rate, and depth-of-cut to enhance performance characteristics in Al6351 alloy plates. The parameters evaluated include surface roughness (Ra), material removal rate (MRR), resultant forces (RF), and temperature at the tool- workpiece interface (Temp). A modified Taguchi method was used to statistically analyze experimental results and develop equations correlating machining parameters with performance outcomes. These equations were validated through experimentation. Additionally, corrections were calculated to estimate each performance characteristic minimum and maximum values under varying conditions. The optimal parameter combination were cutting speed of 1130 rpm, feed rate of 400 mm/min, and depth-of-cut of 0.15 mm, which was found to simultaneously achieve low Ra, high MRR, low RF, and low Temp. All analyses were performed using Microsoft Excel. The results from the modified Taguchi approach were comparable to those obtained from heuristic intelligence algorithms. These studies will be easily extended to AA6351/Al_2O_3 metal matrix composites through stir casting methods useful in automotive and other sectors.

Keywords: Machining parameters optimization, modified Taguchi method, surface roughness (RA), material removal rate (MRR), Al6351 alloy machining, multi-objective optimization

***Author for Correspondence**
Suthapalli Satya Surya Sai Lokesh

[1,2]Student, Department of Mechanical Engineering, Koneru Lakshmaiah Education Foundation, Green Fields, Vaddeswaram, Guntur, Andhra Pradesh, India
[3]Professor, Department of Mechanical Engineering, Koneru Lakshmaiah Education Foundation, Green Fields, Vaddeswaram, Guntur, Andhra Pradesh, India
[4]Post Doctoral Fellow, Department of Mechanical Engineering, School of Engineering and Applied Sciences, SRM University AP, Amaravati, Andhra Pradesh, India
[5]Student, George W. Woodruff School of Mechanical Engineering, Georgia Institute of Technology, Atlanta- 30332, Georgia, USA
[6]Assistant Professor, Department of Mechanical Engineering, School of Engineering, ANURAG University, Ghatkesar, Hyderabad, Telangana, India

Received Date: September 13, 2025
Accepted Date: September 29, 2025
Published Date: May 01, 2026

Citation: Suthapalli Satya Surya Sai Lokesh, K. Sri Manikanta, Boggarapu Nageswara Rao, K. Prasanth Kumar Reddy, V. Sai Akshara, Muni Tanuja Anantha. Experimental Investigation and Optimization of Machining Parameters for Al6351 Alloy Using a Modified Taguchi Approach. Journal of Polymer & Composites. 2026; 14(Special Issue 2): S1463–S1481p.

INTRODUCTION

Machining, a subtractive manufacturing process, achieves desired part shapes by precisely removing material from a workpiece. The challenge lies in simultaneously optimizing several factors: maintaining tight dimensional tolerances, ensuring desired surface integrity and roughness, and maximizing material removal rate (MRR), all while adhering to machine tool capabilities and dynamic constraints. Economic efficiency in machining heavily depends on minimizing production costs by increasing production rate, which is inversely proportional to production time. Various techniques, including CNC milling, end milling, high-speed machining, plunge milling, and cryogenic machining, each offer specific advantages, based on part complexity, surface finish requirements, and production volume. Achieving high-quality results requires balancing conventional and non-conventional methods and strategically optimizing key parameters [1]. A solid understanding of material properties and the impact of different machining strategies is therefore essential for effective processing. Industries like aerospace, automotive, medical device manufacturing, electronics, and defense significantly benefit from advanced machining techniques, leveraging their ability to deliver precision, efficiency, and complex geometries to meet modern manufacturing demands.

Key machining parameters include spindle speed (cutting tool rotation), feed rate (workpiece movement speed), depth of cut (material removed per pass), and tool geometry (rake angle, clearance angle, material). Techniques like Response Surface Methodology (RSM) model and optimize these parameters to minimize cutting force and surface roughness [2]. The Taguchi Method identifies optimal parameters by analyzing their influence on surface roughness and other responses [3, 4]. Grey Relational Analysis (GRA) enables multi-response optimization by combining multiple performance characteristics into a single metric [5–11]. Finite Element Simulations predict the impact of machining parameters on cutting forces, temperature, and stress distribution [12, 13]. Typical parameter ranges [4, 13, 14] include spindle speeds (1500–6000 rpm), feed rates (0.08-0.5 mm/rev), and depths of cut (0.2–4.99 mm), varying based on alloy and desired outcomes. Effective tool geometry may incorporate a 17.95° rake angle and 2° clearance angle [13]. Minimizing surface roughness (Ra) is a primary objective, achieved through careful parameter selection [2, 3, 15]. A high MRR is desirable for efficiency but requires a balanced optimization of speed, feed, and depth of cut [5, 16]. Lower cutting forces and temperatures are also beneficial, as they reduce tool wear and workpiece deformation [13, 15]. Optimizing machining parameters for aerospace aluminum alloys can lead to significant reductions in production costs and improved part quality [4, 14]. This process is complex, involving consideration of various key parameters, challenges, and advanced optimization techniques [16, 17]. The selection of tool material is crucial for optimizing machining parameters, directly affecting tool wear [18], machining efficiency [19, 20], surface quality, and energy consumption [21].

Milling of Al6351 Alloy Plates

A significant amount of research focuses on multi-objective optimization and incorporating environmental impact assessments to improve manufacturing efficiency and quality. Aluminum alloy 6351 (Al 6351) is a widely used material in applications like pressure vessel cylinders, aerospace components, automotive parts, boat hulls, structural columns, chimneys, rods, molds, pipes, and tubes. Its popularity stems from its low weight, high strength, excellent corrosion resistance, toughness, resistance to low-ductility fracture, and good fabricability. Hema et al. [22] experimentally investigated the milling of Al 6351 alloy plates to identify optimal machining parameters. They employed a Hybrid Artificial Bee Colony (HABC) algorithm to minimize process responses and compared its performance to the Harmony Search Algorithm (HSA), Particle Swarm Optimization (PSO), and Genetic Algorithm (GA). The results demonstrated that the HABC algorithm achieved superior solution quality. Multi-objective optimization was accomplished using a composite objective function with equal weights assigned to each objective. The HABC algorithm was then used to determine the optimized milling parameters. Confirmatory experiments showed good agreement between predicted and experimentally obtained results.

Objective of the Present Study

This study optimizes machining parameters (cutting speed, feed rate, and depth-of-cut) for Al6351 alloy plates to achieve desired surface roughness (Ra), material removal rate (MRR), resultant forces (RF), and tool-workpiece interface temperature (Temp). A modified Taguchi method is used to develop empirical relationships between these performance characteristics and input variables, validated against experimental data. These relationships are then used to predict the upper and lower bounds of Ra, MRR, RF, and Temp. Excel-based computations demonstrate that the modified Taguchi method outperforms heuristic intelligence algorithms like HSA, PSO, GA, and HABC.

Journal of Polymer & Composites
Volume 14, Special Issue 2
ISSN: 2321-2810 (Online), ISSN: 2321-8525 (Print)

MATERIALS AND METHODS

In their investigation, Hema et al. [22] experimentally examined the milling process of Al6351 alloy plates, aiming to find the ideal machining parameters. They used a plate with dimensions of 100 mm in length, 50 mm in width, and 32 mm in thickness. The objective was to optimize cutting speed, feed rate, and depth-of-cut to achieve desired performance characteristics. These characteristics included surface roughness (Ra), material removal rate (MRR), resultant forces (RF), and temperature (Temp). The Al6351 alloy used in their study has a specific chemical composition: 97.51% aluminum (Al), 0.8% silicon (Si), 0.75% magnesium (Mg), 0.52% manganese (Mn), 0.12% iron (Fe), 0.017% titanium (Ti), 0.006% zinc (Zn), 0.05% copper (Cu), and 0.14% other elements. They used a Horizontal Milling Machine (Model: HMT FN-U) for the milling operations (see Figure 1).

A milling tool dynamometer was integrated with the milling machine to measure the forces generated during the machining process (see Figure-2). The cutting tool had a diameter of 75 mm, and the high-speed steel (HSS) cutter diameter was 65 mm. Kerosene was used as the coolant during the machining. Surface roughness was measured using a Talysurf instrument. To calculate the material removal rate (MRR), the workpiece was weighed before (w_i) and after (w_f) the cutting operations. MRR was calculated using the formula:

$$MRR = \frac{(w_i - w_f)}{\rho \times t}, \quad (1)$$

where w_i and w_f are the initial and final weights in grams, ρ is the density of the die steel (0.00271 g/mm³), and t is the machining time in seconds. A temperature gun was used to monitor the temperature at the tool- workpiece contact point during the milling operations.

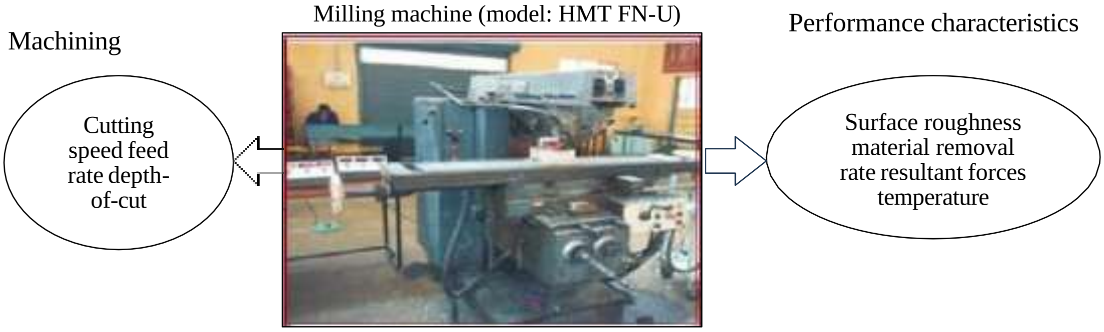

Figure 1. Experimental setup for milling of Al6351 alloy plates [22].

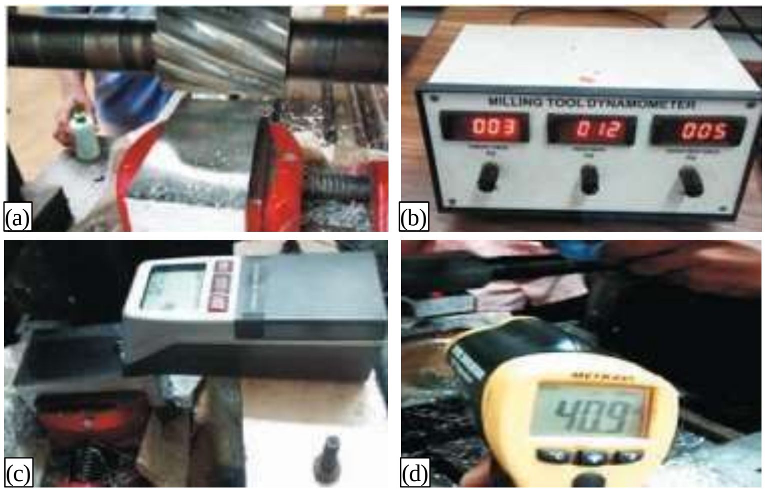

Figure 2. Instruments for measuring performance characteristics in milling of Al6351 alloy plates. (a) HSS cutter and al6351 workplace with milling too; (b) Dynamometer; (c)Tal surf – surface roughness measurement meter; (d) Temperature gun [22].

Table 1. Levels of input parameters.

Input parameters	Designation	Level: 1	Level: 2	Level: 3
Cutting Speed (rpm)	S	730	900	1130
Feed Rate (mm/min)	F	400	630	800
Depth-of-cut (mm)	DOC	0.15	0.25	0.35
Dummy	DP	ε_1	ε_2	ε_3

Table 2. Levels and sets of input variables as per the Taguchi's L9 OA.

Levels of Input Variables					Sets of Input Variables			
Set No.	S	F	DOC	DP	Cutting Speed, S (rpm)	Feed Rate, F(mm/min)	Depth of cut, DOC (mm)	Dummy, DP
1	1	1	1	1	730	400	0.15	ε_1
2	1	2	2	2	730	630	0.25	ε_2
3	1	3	3	3	730	800	0.35	ε_3
4	2	1	2	3	900	400	0.25	ε_3
5	2	2	3	1	900	630	0.35	ε_1
6	2	3	1	2	900	800	0.15	ε_2
7	3	1	3	2	1130	400	0.35	ε_2
8	3	2	1	3	1130	630	0.15	ε_3
9	3	3	2	1	1130	800	0.25	ε_1

To achieve high-performance machining, a modified Taguchi method along with a reliable multi-objective optimization technique is utilized in the optimal solution, whose details are as follows.

To perform the milling process of Al6351 alloy plates, each input parameter in Table 1 is assigned with 3 levels. Taguchi' L9 OA (orthogonal array) is considered for conducting fewer experiments and set the input parameters for each test run. For n_l = 3 levels to each input parameter, the number of input parameters (n_p) according to the Taguchi's L9 OA can be found from [23]

$$N_{Tag} = 1 + n_p(n_l - 1) \Rightarrow n_p = \frac{(N_{Tag}-1)}{(n_l-1)} = \frac{(9-1)}{(3-1)} = \frac{8}{2} = 4 \quad (2)$$

For N_{Tag} =9 tests, 4 input parameters can be accommodated. In this case, only 3 input parameters (i.e. S, F, and DOC) were set and hence, a dummy (fictitious) parameter is introduced i.e. DP in Table-1 to assess the error in estimates for output responses. This aspect was thoroughly discussed in [24]. Measured data of milling process for the 9 sets of input parameters are tabulated in Table 2.

An analysis of variance (ANOVA) was performed on the performance characteristic data (Table 3), and the summarized results are presented in Table 3. The ANOVA results (Table 3) reveal the dominant factors influencing each performance characteristic. Specifically, feed rate (F) accounts for the largest portion of variance in surface roughness (Ra) at 45.45%. Depth-of-cut (DOC) has the most significant impact on material removal rate (MRR), contributing 48.3%. Cutting speed (S) is the primary influencer of resultant forces (RF), explaining 42.7% of the variance. Finally, DOC contributes the most to the temperature at the tool-workpiece contact point (Temp), with a contribution of 78.7%.

The contributions of the other parameters are as follows: For Ra, cutting speed (S) and DOC contribute 13.3% and 40%, respectively. Regarding MRR, cutting speed (S) and feed rate (F) contribute 14.7% and 36.8%, respectively. For RF, feed rate (F) and DOC contribute 18.1% and 37.8%, respectively. The proportions of S and F on Temp are 17.9% and 3.2%, respectively. The contributions from the three process variables (S, F, and DOC) and a fictitious parameter (DP) sum to 100% for each performance characteristic (Ra, MRR, RF, and Temp). This fictitious parameter, DP, accounts for 1.3% of the variance in Ra, 0.2% in MRR, 1.3% in RF, and 0.2% in Temp.

Table 3. Performance characteristics including surface roughness (Ra), material removal rate (MRR), resultant forces (RF) and temperature (temp) in milling of AL6351 for the sets of input variables as per the Taguchi's L9 OA.

Set No.	Performance Characteristics [22]			
	Ra (μm)	***MRR (mm3/sec)***	***RF (N)***	***Temp (°C)***
1	0.1	39.07	13.74	30.1
2	0.155	45.005	15.78	34.95
3	0.22	49.2	18.78	40.6
4	0.127	43.211	13.43	35.9
5	0.21	47.97	15.74	41.6
6	0.17	45.1	13.6	33.1
7	0.13	47.75	13.34	42.6
8	0.1	44.28	12.08	35.3
9	0.17	50.225	13.98	40.2

Experimentation is often essential in manufacturing to observe phenomena before developing mathematical models. Unidentified influences, including measurement errors, can lead to performance variations in repeated tests. Although Taguchi's L9 orthogonal array (OA) is designed for four parameters at three levels, this study used only three parameters at three levels. To maintain the applicability of ANOVA, a fictitious fourth parameter (DP) was introduced, allowing for the calculation of percentage contributions. The DP parameter can be interpreted as an unidentified influencing factor, or even measurement errors affecting the performance characteristics.

Experimentation is often essential in manufacturing to observe phenomena before developing mathematical models. Unidentified influences, including measurement errors, can lead to performance variations in repeated tests. Although Taguchi's L9 orthogonal array (OA) is designed for four parameters at three levels, this study used only three parameters at three levels. To maintain the applicability of ANOVA, a fictitious fourth parameter (DP) was introduced, allowing for the calculation of percentage contributions. The DP parameter can be interpreted as an unidentified influencing factor, or even measurement errors affecting the performance characteristics.

The modified Taguchi method, as detailed in references [25–33], allows for the determination of the expected range of performance characteristics, specifically Ra, MRR, RF, and Temp, within a defined operational space. By considering the designated process parameters (S, F, and DOC), this method facilitates process design by providing insight into the anticipated variability one might observe in repeated experiments. Using either Ra or MRR or RF or Temp, as the performance measure (φ), and applying the additive law [23], Equation (3) enables the estimation of the performance measure (φ^e) based on the levels of the input variables.

$$\varphi^e = \varphi_g^m + \sum_{i=1}^{n_p}(\varphi_{il}^m - \varphi_g^m) = \sum_{i=1}^{n_p}\varphi_{il}^m - (n_p - 1)\varphi_g^m \qquad (3)$$

Equation (3)'s components can be obtained from ANOVA Table 4. The subscript 'i' combined with $i = 1,2,3,4$ refers to the milling process parameters (S, F, DOC, and DP), while 'l' combined with $l = 1,2,3$ represents the 1-, 2-, or 3-mean of Ra or MRR or RF or Temp at the corresponding levels of those parameters. φ_g^m is the grand mean of the performance measure across all nine test runs. For example, when considering Ra as the performance measure, $\varphi_g^m = Ra_g^m = 0.1536\mu m$ and $\varphi_{22}^m = Ra_{22}^m = 0.1550\mu m$ (as seen in ANOVA Table 4. This $0.1550\mu m$ value corresponds to the 2-mean of Ra at level 2 of the milling process parameter F. The estimated Ra, MRR, RF, and Temp values from Table 4 are used for comparison with the experimentally obtained results from the Taguchi L9OA. When n_p =4 and n_p =3 are applied in Equation (3), the performance characteristics are estimated both with and without the influence of parameter DP, respectively. It is clear from Tables 5–8 that a discrepancy exists in the estimates when n_p=3. However, when n_p =4, the estimates match the test data.

Table 4. ANOVA results showing the significance of input variables on the performance characteristics (such as Ra, MRR, RF, and temp).

Input variables	1st mean	2nd mean	3rd mean	SOS (Sum of squares)	%Contribution
Surface roughness (Ra): Grand mean, Ra_g^m= 0.1536μm					
S	0.1583	0.1690	0.1333	2.011E-03	13.3
F	0.1190	0.1550	0.1867	6.877E-03	45.4
DOC	0.1233	0.1507	0.1867	6.054E-03	40.0
DP	0.1583	0.1690	0.1333	1.975E-04	1.3
Material Removal Rate (MRR): Grand mean, MRR_g^m= 45.7568 mm3/sec					
S	44.4250	45.4269	47.4183	13.930	14.7
F	43.3436	45.7517	48.1750	35.014	36.8
DOC	42.8167	46.1469	48.3067	45.895	48.3
DP	45.7550	45.9517	45.5636	0.226	0.2
Resultant forces (RF): Grand mean, RF_g^m= 14.4967 N					
S	16.1000	14.2567	13.1333	1.346E+01	42.7
F	13.5033	14.5333	15.4533	5.710E+00	18.1
DOC	13.1400	14.3967	15.9533	1.192E+01	37.8
DP	14.4867	14.2400	14.7633	4.113E-01	1.3
Temperature (Temp): Grand mean, $Temp_g^m$= 37.1500°C					
S	35.2167	36.8667	39.3667	26.195	17.9
F	36.2000	37.2833	37.9667	4.762	3.2
DOC	32.8333	37.0167	41.6000	115.362	78.7
DP	37.3000	36.8833	37.2667	0.322	0.2

Table 5. Estimates of surface roughness, Ra (μm).

Set No.	Test [22]	Estimate Eq. (3)			Estimated range	
		$n_p = 3$	*R.E (%)*	$n_p = 4$	*From*	*To*
1	0.1	0.0936	6.4	0.100	0.0890	0.1000
2	0.155	0.1569	-1.2	0.155	0.1523	0.1633
3	0.22	0.2246	-2.1	0.220	0.2200	0.2310
4	0.127	0.1316	-3.6	0.127	0.1270	0.1380
5	0.21	0.2036	3.0	0.210	0.1990	0.2100
6	0.17	0.1719	-1.1	0.170	0.1673	0.1783
7	0.13	0.1319	-1.5	0.130	0.1273	0.1383
8	0.1	0.1046	-4.6	0.100	0.1000	0.1110
9	0.17	0.1636	3.8	0.170	0.1590	0.1700

Table 6. Estimates of material removal rate, MRR (mm3/sec).

Set No.	Test [22]	Estimate Eq. (3)			Estimated range	
		$n_p = 3$	*R.E (%)*	$n_p = 4$	*From*	*To*
1	39.07	39.072	0.0	39.070	38.879	39.267
2	45.005	44.810	0.4	45.005	44.617	45.005
3	49.2	49.393	-0.4	49.200	49.200	49.588
4	43.211	43.404	-0.4	43.211	43.211	43.599
5	47.97	47.972	0.0	47.970	47.779	48.167
6	45.1	44.905	0.4	45.100	44.712	45.100
7	47.75	47.555	0.4	47.750	47.362	47.750
8	44.28	44.473	-0.4	44.280	44.280	44.668
9	50.225	50.227	0.0	50.225	50.034	50.422

Journal of Polymer & Composites
Volume 14, Special Issue 2
ISSN: 2321-2810 (Online), ISSN: 2321-8525 (Print)

Table 7. Estimates of resultant forces, RF (N).

Set No.	Test [22]	Estimate Eq. (3)			Estimated range	
		$n_p = 3$	*R.E (%)*	$n_p = 4$	*From*	*To*
1	13.74	13.750	-0.1	13.740	13.493	14.017
2	15.78	16.037	-1.6	15.780	15.780	16.303
3	18.78	18.513	1.4	18.780	18.257	18.780
4	13.43	13.163	2.0	13.430	12.907	13.430
5	15.74	15.750	-0.1	15.740	15.493	16.017
6	13.6	13.857	-1.9	13.600	13.600	14.123
7	13.34	13.597	-1.9	13.340	13.340	13.863
8	12.08	11.813	2.2	12.080	11.557	12.080
9	13.98	13.990	-0.1	13.980	13.733	14.257

Table 8. Estimates of temperature, Temp (°C).

Set No.	Test [22]	Estimate Eq. (3)			Estimated range	
		$n_p = 3$	*R.E (%)*	$n_p = 4$	*From*	*To*
1	30.1	29.950	0.5	30.100	29.683	30.100
2	34.95	35.217	-0.8	34.950	34.950	35.367
3	40.6	40.483	0.3	40.600	40.216	40.633
4	35.9	35.783	0.3	35.900	35.516	35.933
5	41.6	41.450	0.4	41.600	41.183	41.600
6	33.1	33.367	-0.8	33.100	33.100	33.517
7	42.6	42.867	-0.6	42.600	42.600	43.017
8	35.3	35.183	0.3	35.300	34.916	35.333
9	40.2	40.050	0.4	40.200	39.783	40.200

Corrections are applied to the n_p=3 estimates by determining the minimum and maximum deviations of the mean values, related to the dummy parameter DP, from the overall grand mean. Applying these corrections to the estimates allows for the determination of the estimated range of performance characteristics. By applying the respective corrections of -0.0046 µm, -0.1932 mm3/sec, -0.2567 N, and -0.2667 °C to the estimates of Ra, MRR, RF, and Temp, the lower bound values are obtained. Conversely, upper bound values for Ra, MRR, RF, and Temp are obtained by applying the respective corrections of 0.0064 µm, 0.1949 mm3/sec, 0.2667N, and -0.1500 °C, to their corresponding estimates.

To show how straightforward this analysis is, the Ra estimates from Test Run-1 in Table-5 are detailed below. In Test Run-1, the levels for factors S, F, DOC, DP were set to 1 (1, 1, 1, 1). The average Ra values, as determined from ANOVA Table-4,were: $\varphi^m_{11} = Ra^m_{11} = 0.1583\mu m$; $\varphi^m_{21} = Ra^m_{21} = 0.1190\mu m$;$\varphi^m_{31} = Ra^m_{31} = 0.1233\mu m$; and $\varphi^m_{41} = Ra^m_{41} = 0.1600\mu m$. The overall average (grand mean),φ^m_g=Ra^m_g= $0.1536\mu m$.

First, let us calculate Ra for Test Run-1 excluding factor DP (i.e., $n_p = 3$). Using Equation (3), one gets:

$$Ra^e = Ra^m_{11} + Ra^m_{21} + Ra^m_{31} - 2 \times Ra^m_g = 0.1583+0.1190+0.1233-2\times0.1536=0.0936\mu m$$

Next, let us calculate Ra for Test Run-1 including factor DP (i.e., n_p=4). Using Eq. (3), one gets:

$$Ra^e = Ra^m_{11} + Ra^m_{21} + Ra^m_{31} + Ra^m_{41} - 3 \times Ra^m_g = 0.1583+0.1190+0.1233+0.1600-3\times0.1536=0.1\mu m$$

The corrections applied to the Ra estimates (when factor DP is excluded) are based on the minimum and maximum deviations of the mean values associated with factor DP from the overall average:

$$min\{Ra^m_{41}, Ra^m_{42}, Ra^m_{43}\} - Ra^m_g = min\{0.1600,\ 0.1517,\ 0.1490\}\text{-}0.1536$$
$$= 0.1490\text{-}0.1536 = \text{-}0.0046\mu m$$

$$max\{Ra^m_{41}, Ra^m_{42}, Ra^m_{43}\} - Ra^m_g = \max\{0.1600,\ 0.1517,\ 0.1490\}\text{-}0.1536$$
$$= 0.1600\text{-}0.1536 = \text{-}0.0064\mu m$$

Applying these corrections to the Ra estimate obtained excluding factor DP, we determine the minimum and maximum Ra estimates for Test Run-1: 0.0890 (=0.0936-0.0046) and 0.1 (=0.0936+0.0064).

For the specific combinations of input parameter levels (SF, and DOC) defined by the Taguchi L9 OA, Ra, MRR, RF, and Temp are evaluated using Equation (3). Appropriate corrections are then applied to establish the lower and upper limits for Ra, MRR, RF, and Temp. The results from Test data [22] in Table 4 fall within this estimated range.

Using this additive law (3), it is possible to estimate the performance characteristics for all combinations of the three levels across the three milling process parameters. A full factorial experimental design was implemented with three input parameters (S, F, and DOC). Three levels were assigned to each parameter resulting 27 distinct experimental conditions (3^3). Each condition identified by its specific parameter level combination. These are $(((S_i, F_j, DOC_k), k = 1 \lesssim to3), j = 1to3), i = 1to3)$ in which subscripts to parameters (S, F, DOC) are the levels. Equation (3) was used to calculate Ra, MRR, RF, and Temp values for all 27 combinations. Figures 3(a)–(d) graphically represent the full factorial design results along with the measured data [22]. Specifically, the parameter combinations corresponding to sequence numbers 1, 5, 9, 11, 15, 16, 21, 22, and 26 were selected to align with the nine runs of Taguchi's L9 OA. The measured data shown in Figures 3(a)–(d) fell within or close to the specified lower and upper limits.

The levels of each process parameter were transformed into coded values (-1 to 1) to create quadratic polynomials representing the mean performance indicator values for Ra, MRR, RF, and Temp (ANOVA Table 4. Applying these polynomials within the additive law framework (equation 3), we derived empirical relationships between Ra, MRR, RF, and Temp and the input variables S, F, and DOC.

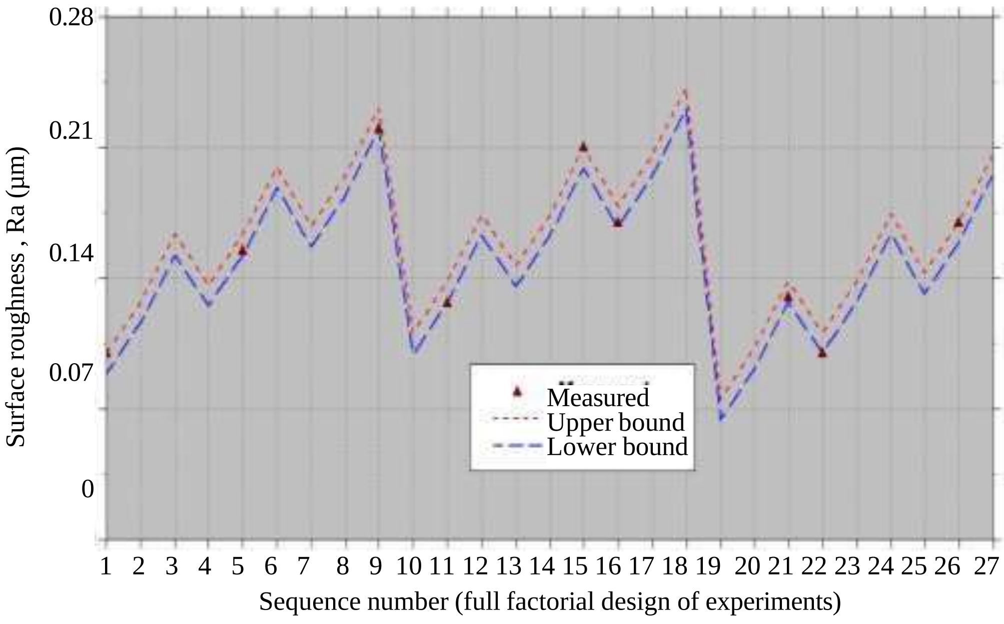

Figure 3. (a) Comparison between measured [22] and Ra estimates.

Journal of Polymer & Composites
Volume 14, Special Issue 2
ISSN: 2321-2810 (Online), ISSN: 2321-8525 (Print)

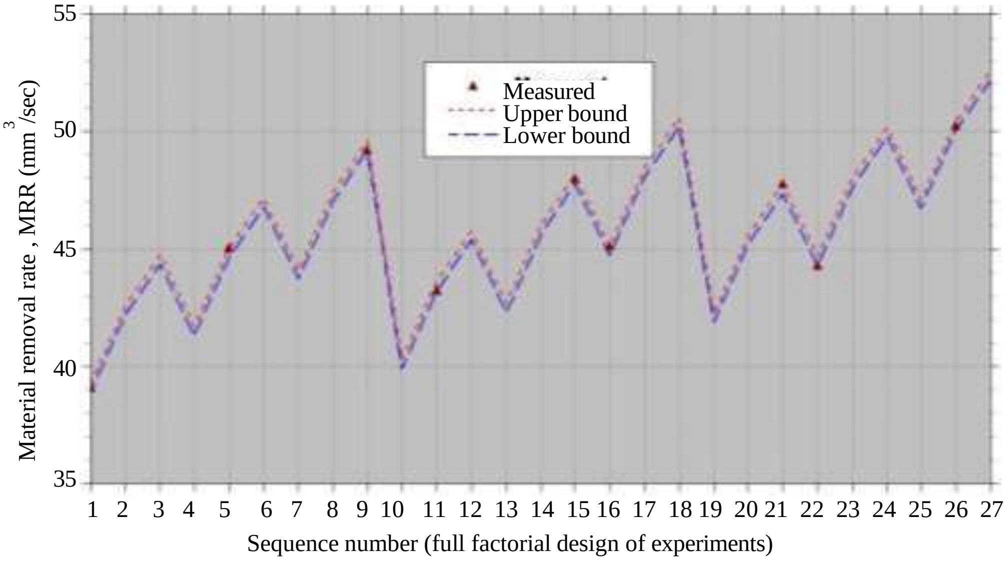

Figure 3. (b) Comparison between measured [22] and MRR estimates.

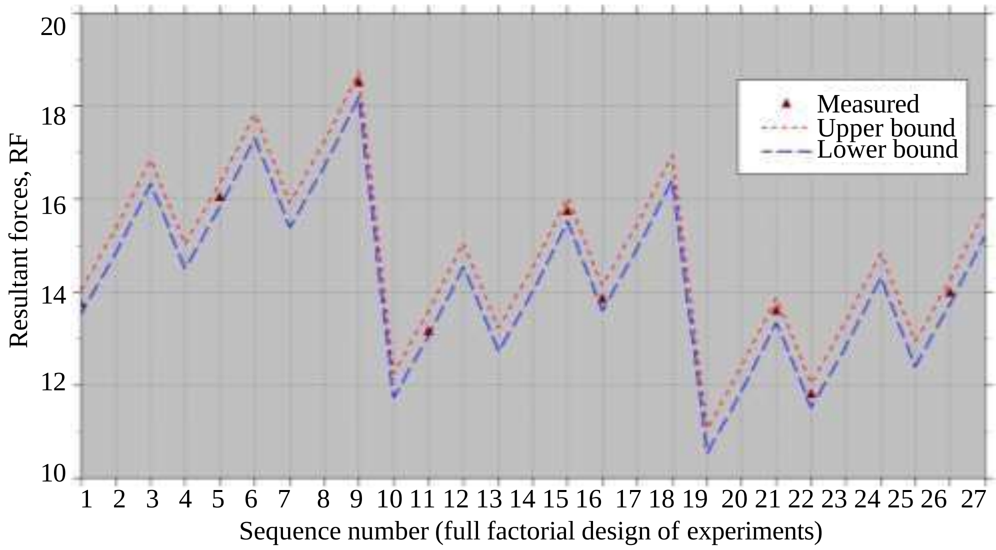

Figure 3. (c). Comparison between measured [22] and RF estimates.

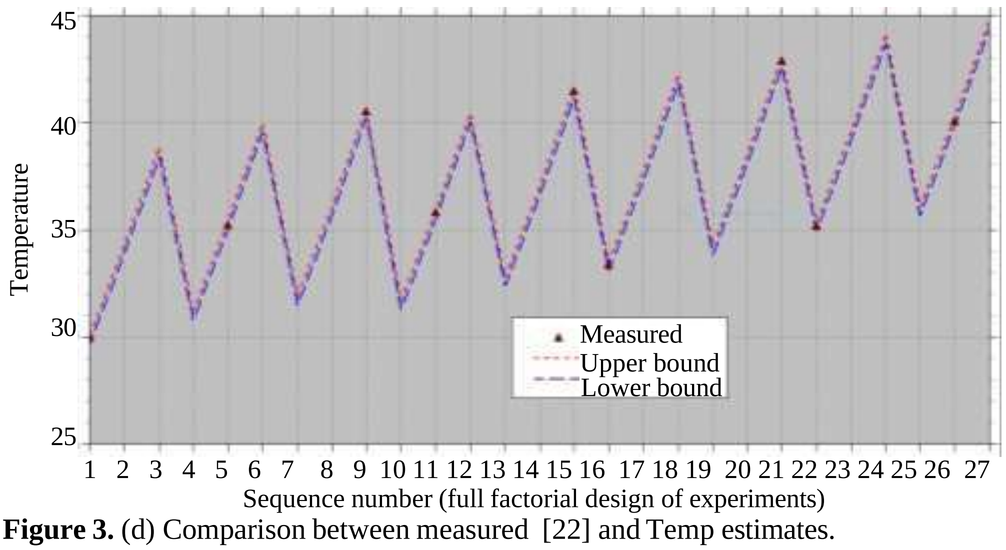

Figure 3. (d) Comparison between measured [22] and Temp estimates.

The coded parameters used were:
$\xi_1 = \frac{1}{200}(S - 930)$; $\xi_2 = = \frac{1}{200}(F - 600)$; and $\xi_3 = 10(DOC - 0.25)$

The following relationships were established using the mean values of Ra, MRR, RF, and Temp from ANOVA Table 4.

$$Ra = 0.1610 - 0.0125\xi_1 - 0.02179\xi_1^2 + 0.0338\xi_2 + 0.00298\xi_2^2 + 0.0317\xi_3 + 0.00433\xi_3^2 \quad (4)$$

$$MRR = 45.6594 + 1.4967\xi_1 + 0.27646\xi_1^2 + 2.4157\xi_2 + 0.3785\xi_2^2 + 2.7450\xi_3 - 0.58526\xi_3^2 \quad (5)$$

$$RF = 13.8091 - 1.4833\xi_1 + 0.59591\xi_1^2 + 0.9750\xi_2 + 0.09335\xi_2^2 + 1.4067\xi_3 + 0.15\xi_3^2 \quad (6)$$

$$Temp = 37.0444 + 2.0750\xi_1 + 0.11637\xi_1^2 + 0.8833\xi_2 - 0.0695\xi_2^2 + 4.3833\xi_3 + 0.2\xi_3^2 \quad (7)$$

In order to illustrate the utility of Equations (4) through (7), we will analyze Test Run-1, which consists of three levels and the parameter values: rotational speed (S) = 730 rpm, feed rate (F) = 400 mm/min, and depth of cut (DOC) = 0.15 mm. The transformed parameters for this particular set are ($\xi_1 = -1$, $\xi_2 =-1$, $\xi_3 = -1$).

Upon substituting these transformed parameters into Equations (4) to (7), we obtain the following results:

Ra = 0.1610 − 0.0125 × (−1) − 0.02179 × $(-1)^2$ + 0.0338 × (−1) + 0.00298 × $(-1)^2$ + 0.0317 × (−1) + 0.00433 × $(-1)^2$ = 0.1610 + 0.0125 − 0.02179 − 0.0338 + 0.00298 − 0.0317 + 0.00433 ≈ 0.0935μm

MRR = 45.6594 + 1.4967 × (−1) + 0.27646 × $(-1)^2$ + 2.4157 × (−1) + 0.3785 × $(-1)^2$ +2.7450 × (−1) − 0.58526 × $(-1)^2$ = 45.6594 − 1.4967 + 0.27646 − 2.4157 + 0.3785 − 2.7450 − 0.58526 ≈ 39.072mm^3/sec

RF = 13.8091 − 1.4833 × (−1) + 0.59591 × $(-1)^2$ + 0.9750 × (−1) + 0.09335 × $(-1)^2$ + 1.4067 × (−1) + 0.15 × $(-1)^2$ = 13.8091 + 1.4833 + 0.59591 − 0.9750 + 0.09335 − 1.4067 + 0.15 ≈ 13.750N

$Temp$ = 37.0444 + 2.0750 × (−1) + 0.11637 × $(-1)^2$ + 0.8833 × (−1) − 0.0695 × $(-1)^2$ + 4.3833 × (−1) + 0.2 × $(-1)^2$ = 37.0444 − 2.0750 + 0.11637 − 0.8833 + −0.0695 − 4.3833 + 0.2 ≈ 29.950^oC

Applying corrections of -0.0046 µm and 0.0064 µm to the Ra values resulted in a range of 0.0889 µm to 0.0999 µm, which aligns well with the data presented in Table 4. Similarly, adjusting the predicted MRR values with corrections of -0.1932 mm³/sec and +0.1949 mm³/sec produced a lower bound of 38.879 mm³/sec and an upper bound of 39.267 mm³/sec, demonstrating good agreement with Table 4. For the predicted RF values, applying corrections of -0.2567 N and +0.2667 N yielded a range of 13.493 N to 14.017 N, again closely matching the results in Table 4. Finally, correcting the predicted Temp values using -0.2667oC and +0.15oC gave a range of 29.683oC to 30.100oC, showing favorable comparison with the findings in Table 4. This overall consistency validates the empirical relationships developed for Ra, MRR, RF, and Temp, as modelled in equations (4) through (7). Furthermore, the results obtained from equations (4) through (7) show a stronger correlation with those calculated using the additive law, represented by equation (3).

RESULTS AND DISCUSSION

Analyzing ANOVA Table 4 enables us to pinpoint particular levels of input variables denoted with subscripts: $S_3F_1DOC_1$ to the lowest surface roughness (Ra); $S_3F_3DOC_3$ to the highest material removal rate (MRR); $S_3F_1DOC_1$ to the lowest resultant forces (RF), and $S_1F_1DOC_1$ to the lowest temperature at the tool- workpiece interface (Temp). These combinations of input variables correspond to sequence number 19 in Figure 3(a), sequence number 27 in Figure-3(b), sequence number 19 in Figure 3(c), and sequence number 1 in Figure 3(d) of the full factorial design of experiments. It is important to note that the parameter sets required to attain these optimal values for Ra, MRR, RF, and Temp are different. To derive a cohesive set of parameters that effectively minimizes Ra, while maximizing MRR, and minimizes both RF and Temp, we apply a method previously discussed in research [24–30]: transforming the multi-objective optimization issue into a single-objective problem. This process entails normalizing the values of Ra, MRR, RF, and Temp from ANOVA Table 3 against their respective maximums$(Ra)_{max}$= 0.2363µm; $(MRR)_{max}$= 52.4651 mm³/sec; $(RF)_{max}$= 18.78 N; and$(Temp)_{max}$= 44.833oC.

By minimizing, ζ_1 $(\equiv \frac{Ra}{(Ra)_{max}})$,$\zeta_2$ $(\equiv 1-\frac{MRR}{(MRR)_{max}})$,$\zeta_3$ $(\equiv \frac{RF}{(RF)_{max}})$and ζ_4 $(\equiv \frac{Temp}{(Temp)_{max}})$,

it is possible to find the minimizes Ra, maximizes MRR, minimize RF, and minimize Temp. Using positive weightsω_1,ω_2, ω_3, and$\omega_4$that sum to 1 ($\omega_1+\omega_2+\omega_3+\omega_4=1$) as detailed in [24–33], we establish a unified objective function aimed at concurrently minimizing Ra; maximizing MRR; and minimizing both RF and Temp:

$$\zeta=\omega_1\zeta_1+\omega_2\zeta_2+\omega_3\zeta_3+\omega_4\zeta_4 \tag{8}$$

The unified multi-objective function (ζ)in equation (8) is a linear combination of

ζ_1 $(\equiv \frac{Ra}{(Ra)_{max}})$,$\zeta_2$ $(\equiv 1-\frac{MRR}{(MRR)_{max}})$, ζ_3 $(\equiv \frac{RF}{(RF)_{max}})$ and ζ_4 $(\equiv \frac{Temp}{(Temp)_{max}})$.

We divide each level of the mean value of Ra in ANOVA Table-4 with $(Ra)_{max}$to obtain the corresponding level of the mean value ofζ_1. Each level of the mean value of MRR in ANOVA Table 4 is divided with $(MRR)_{max}$ and then subtract the resultant value from 1 to obtain the corresponding level of the mean value ofζ_2. Similarly, each level of the mean value of RF in ANOVA Table 4 is divided with $(RF)_{max}$to obtain the corresponding level of the mean values of ζ_3. Also, each level of the mean value of Temp in ANOVA Table 4 is divided with $(Temp)_{max}$, to obtain the corresponding level of the mean values of ζ_4. Table 9 displays the mean values of a unified objective function (ζ) based on various sets of weighing factors (ω_1,ω_2, ω_3,ω_4).

Table 9. Mean values of the single objective function(ζ) in Eq. (8) with different sets of weighing factors (ω_1,ω_2,ω_3,ω_4).

Input variables	1stMean	2ndMean	3rdMean	Optimal Solution
$(Ra)_{min}$: $\omega_1=1, \omega_2=\omega_3=\omega_4=0$				
S	0.6551	0.6992	0.5516	$S_3F_1DOC_1$
F	0.4924	0.6413	0.7723	
DOC	0.5103	0.6234	0.7723	
$(MRR)_{max}$: $\omega_1=0, \omega_2=1, \omega_3=\omega_4=0$				
S	0.1551	0.1361	0.0982	$S_3F_3DOC_3$
F	0.1757	0.1299	0.0838	
DOC	0.1857	0.1224	0.0813	
$(RF)_{min}$: $\omega_1=0, \omega_2=0, \omega_3=1, \omega_4=0$				
S	0.8573	0.7591	0.6993	$S_3F_1DOC_1$
F	0.7190	0.7739	0.8229	
DOC	0.6997	0.7666	0.8495	
$(Temp)_{min}$: $\omega_1=0, \omega_2=0, \omega_3=0, \omega_4=1$				
S	0.7864	0.8232	0.8791	$S_1F_1DOC_1$
F	0.8083	0.8325	0.8478	
DOC	0.7332	0.8266	0.9289	
$(Ra)_{min}$,$(MRR)_{max}$,$(FN)_{min}$ and $(Temp)_{min}$: $\omega_1=\omega_2=\omega_3=\omega_4=\frac{1}{4}$				
S	0.6135	0.6044	0.5571	$S_3F_1DOC_1$
F	0.5489	0.5944	0.6317	
DOC	0.5322	0.5847	0.6580	

Minimum Ra is obtained by minimizing ζ with weighting factors $\omega_1 = 1$, $\omega_2 = \omega_3 = \omega_4 = 0$. Maximum MRR is similarly obtained by minimizing ζ with $\omega_1 = 0$, $\omega_2 = 1$, $\omega_3 = \omega_4 = 0$. Minimum RF is obtained by minimizing ζ with $\omega_1 = 0$, $\omega_2 = 0$, $\omega_3 = 1$, $\omega_4 = 0$. Minimum Temp is obtained by minimizing ζ with $\omega_1 = 0$, $\omega_2 = 0$, $\omega_3 = 0$, $\omega_4 = 1$. These four cases were indicated with bold numerals in ANOVA Table-9. The optimal solution for these four cases confirms the data in ANOVA Table-4. To achieve a unified process optimization, the equal weighting factors ($\omega_1 = \omega_2 = \omega_3 = \omega_4 = \frac{1}{4}$) are utilized. Table 10 offers a comprehensive list of specific input variables along with the estimates of the performance characteristics (Ra, MRR, RF, and Temp) for each condition. The measured performance characteristics for each specific condition in Table-10 are within or close to the estimated range.

Hema et al. [22], similar to this study, employed multi-objective optimization, creating a composite objective function where each objective was weighted equally. Using 18 different combinations of input variables (S, F, and DOC), they developed regression model (9) based on measured performance characteristics: Ra, MRR, RF, and Temp.

$$\begin{Bmatrix} Ra \\ MRR \\ RF \\ Temp \end{Bmatrix} = \begin{Bmatrix} 0.0328877 \\ 23.9621 \\ 14.2701 \\ 13.1982 \end{Bmatrix} + \begin{bmatrix} -0.00006450.0001481390.371667 \\ 0.007171990.012538431.1141 \\ -0.006650740.0046179514.0344 \\ 0.0111330.0047146443 \end{bmatrix} \times \begin{Bmatrix} S \\ F \\ DOC \end{Bmatrix} \quad (9)$$

They then used the HABC algorithm to optimize milling parameters and asserted its superiority by comparing its performance against HSA, PSO, and GA (Table 11). Notably, the optimal milling parameter set identified in this study aligns precisely with the results obtained by Hema et al. [22] using HABC algorithm (Tables 6 and 7). Furthermore, the measured performance characteristics reported in [22], along with their estimates derived from regression model (9) for the optimal parameter set, fall within or near to the predicted range. The performance characteristics (Ra, MRR, RF, and Temp) were measured and compared with estimates from the regression model (9), as shown in Figures 4(a)–(d). The regression model (9) provides accurate estimations, with its results falling within or close to the predicted range derived from the empirical relationships (4) to (7).

Table 10. Input variables (such as S, F, and DOC) and the predictions of the performance characteristics (such as Ra, MRR, RF, and Temp) under particular conditions.

Optimal set of input variables			**Performance characteristics**			
S (rpm)	***F (mm/min)***	***DOC (mm)***	***Ra (µm)***	***MRR (mm3/sec)***	***FN (N)***	***Temp (°C)***
Single objective optimization – $(Ra)_{min}$						
1130	400	0.15	0.0639–0.0749 (0.07) +	41.872-42.260 (41.51)	10.527-11.050 (10.95)	33.833–34.250 (34.6)
Single objective optimization - $(MRR)_{axn}$:						
1130	800	0.35	0.1949-0.2059 (0.21)	52.193-52.581 (55.35)	15.290-15.813 (14.96)	44.367-44.783 (44.5)
Single objective optimization - $(RF)_{min}$						
1130	400	0.15	0.0639-0.0749 (0.07)	41.872-42.260 (41.51)	10.527-11.050 (10.95)	33.833-34.250 (34.6)
Single objective optimization - $(Temp)_{min}$						
730	400	0.15	0.0889-0.0999(0.1)	38.879-39.267 (39.07)	13.493-14.017 (13.74)	29.683-30.100 (30.1)
Multi-objective optimization – $(Ra)_{min}$,$(MRR)_{max}$,$(RF)_{min}$and $(Temp)_{min}$						
1130	400	0.15	0.0639-0.0749 (0.07)	41.872-42.260 (41.51)	10.527-11.050 (10.95)	33.833-34.250 (34.6)
+ Test data [22] in parenthesis						

Table 11. Comparison of milling parameters and performance characteristics adopting different heuristic intelligence algorithms (HSA, PSO, GA, HABC) in the multi-objective optimization.

Heuristic intelligence Algorithm	Optimal set of input variables			Performance characteristics (Eq. 9)			
	S (rpm)	*F (mm/min)*	*DOC (mm)*	*Ra (μm)*	*MRR (mm3/sec)*	*FN (N)*	*Temp (°C)*
GA	1057.52	400	0.15	0.080	41.229	11.189	33.307
HSA	1096.11	400	0.15	0.077	41.506	10.932	33.737
PSO	1035.14	406.1	0.16	0.086	41.456	11.507	33.517
HABC	1130	400	0.15	0.075	41.749	10.707	34.114

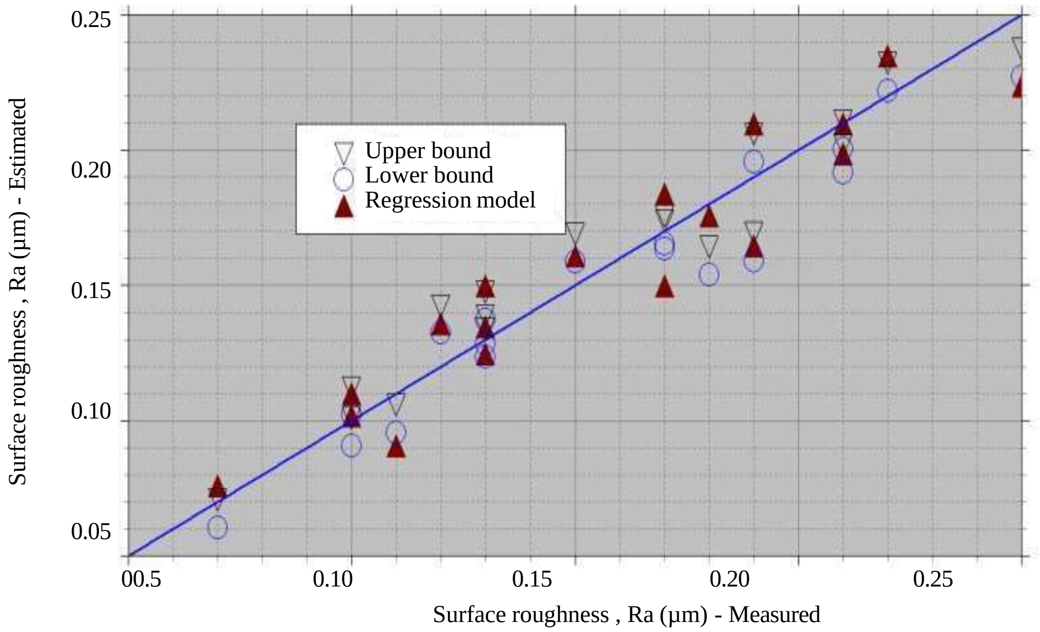

Figure 4. (a) Comparison of measured and estimated surface roughness (Ra) from regression model (9) and the empirical relationship (4).

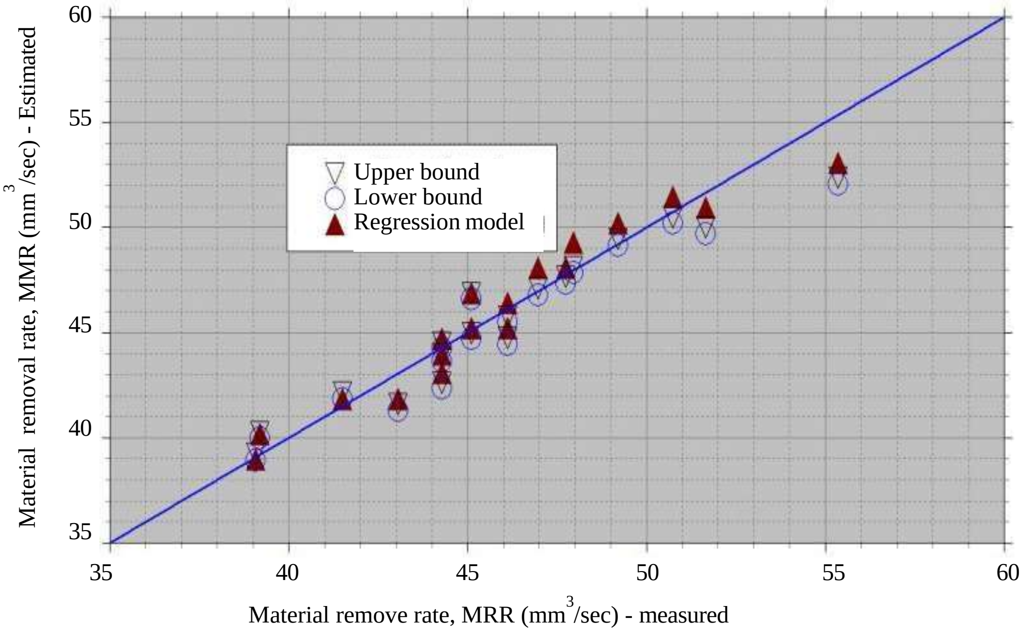

Figure 4. (b) Comparison of measured and estimated material removal rate (MRR) from regression model (9) and the empirical relationship (5).

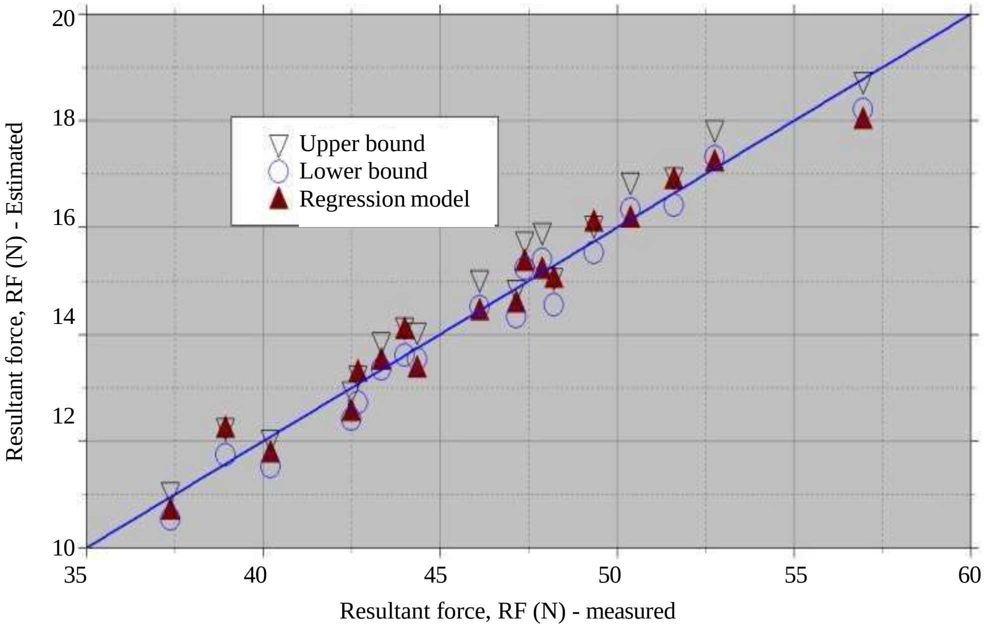

Figure 4. (c) Comparison of measured and estimated resultant forces (RF) from regression model (9) and the empirical relationship (6).

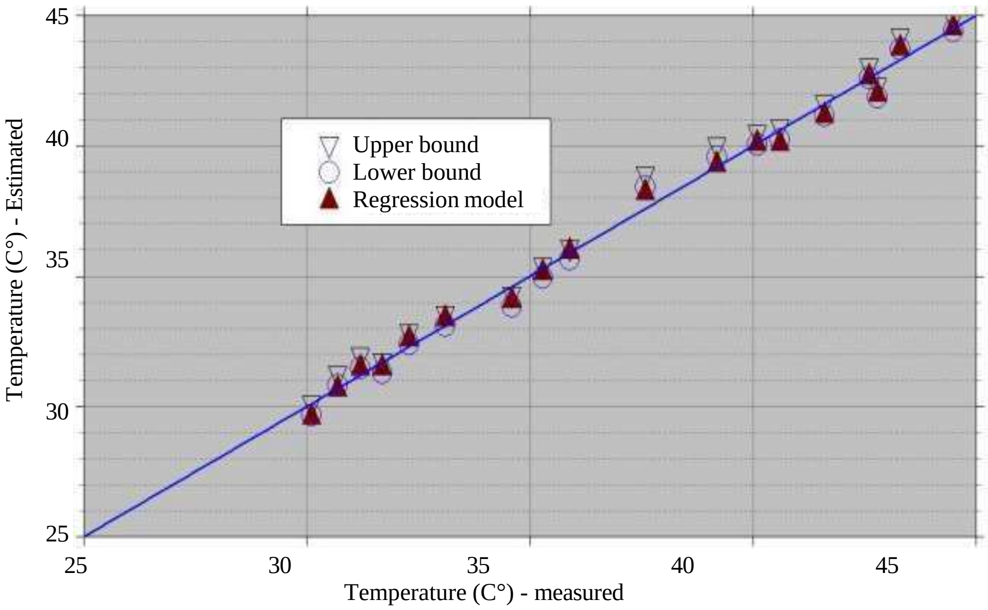

Figure 4. (d) Comparison of measured and estimated temperature (Temp) from regression model (9) and the empirical relationship (7).

Figures 5(a)–(d) illustrate the relationship between cutting speed (S) and several performance characteristics: surface roughness (Ra), material removal rate (MRR), resulting forces (RF), and temperature at the tool-workpiece interface (Temp). These Figures present data collected while maintaining a constant feed rate (F1 = 400 mm/min) and depth-of-cut (DOC1 = 0.15 mm). As cutting speed (S) increases, surface roughness (Ra) initially rises before subsequently declining (Figure 5(a)). In contrast, material removal rate (MRR) (Figure 5(b)) and temperature (Temp) (Figure 5(d)) both demonstrate a consistent increase with increasing cutting speed (S). The resulting forces (RF) (Figure 5(c)) show the opposite trend, decreasing consistently as cutting speed (S) increases. These curves in Figures 5(a) through 5(d) were generated using empirical equations (4) to (7), which were adjusted to account for the upper and lower bounds of the developed empirical relationships.

The industrial sector demands simple, reliable, and easily implemented solutions for optimization problems. This study addresses this need by employing a modified Taguchi method for process optimization, identifying optimal ranges for performance characteristics based on specific process variables. Furthermore, we developed and validated empirical models for Ra, MRR, RF, and Temp using experimental data. Statistical analysis was performed using Excel, offering an alternative to specialized software like Minitab or Design Expert. Importantly, our identified optimal milling parameter set coincides with the findings of Hema et al. [22], who utilized the HABC algorithm and demonstrated its effectiveness over other optimization algorithms, such as HSA, PSO, and GA.

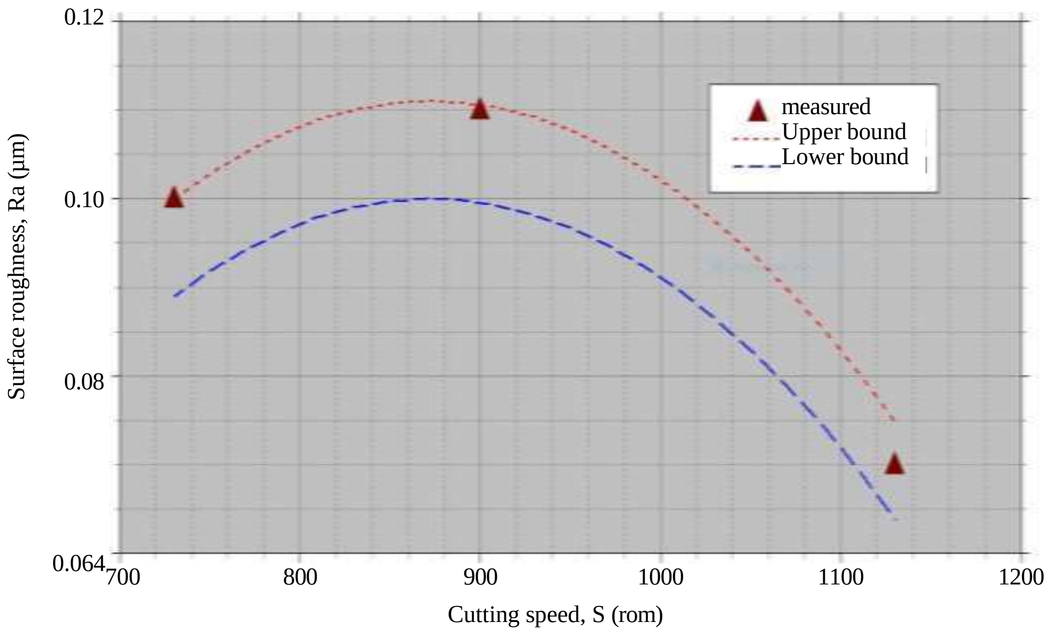

Figure 5 (a) Variation of surface roughness (Ra) with the cutting speed (S) for a given feed rate, F1=400 mm/min and depth-of-cut, DOC1=0.15 mm

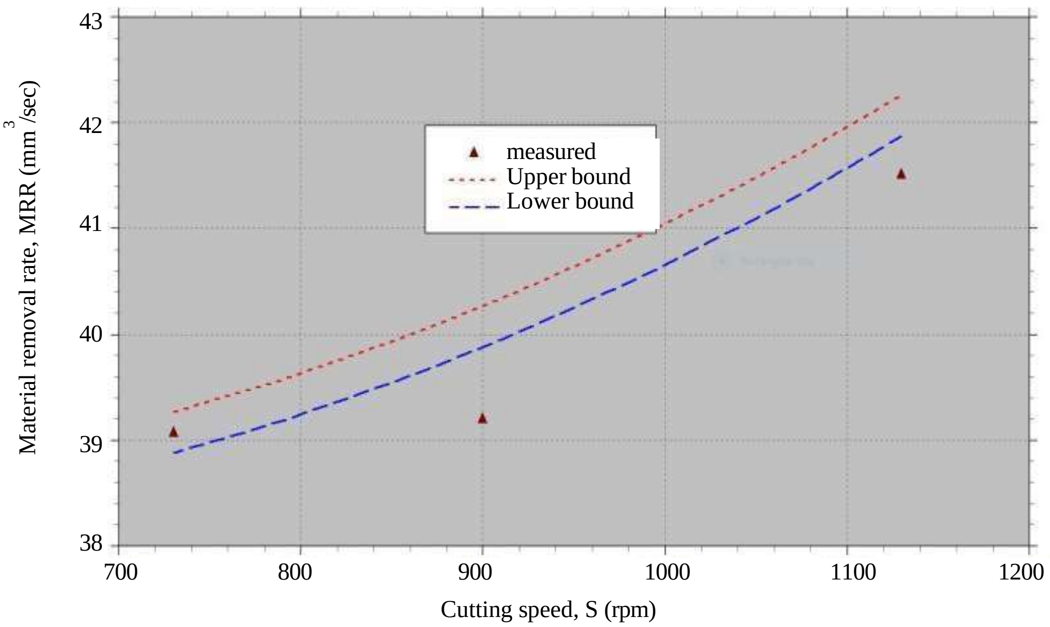

Figure 5. (b) Variation of material removal rate (MRR) with the cutting speed (S) for a given feed rate, F1=400 mm/min and depth-of-cut, DOC1=0.15 mm

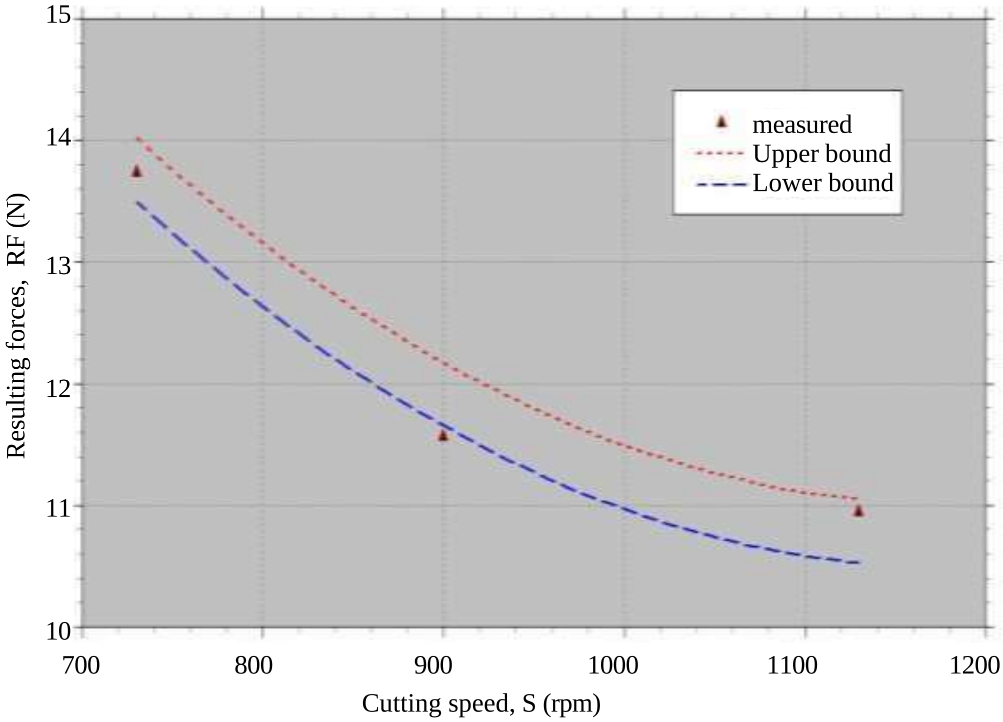

Figure 5. (c) Variation of resulting forces (RF) with the cutting speed (S) for a given feed rate, F1=400 mm/min and depth-of-cut, DOC1=0.15 mm

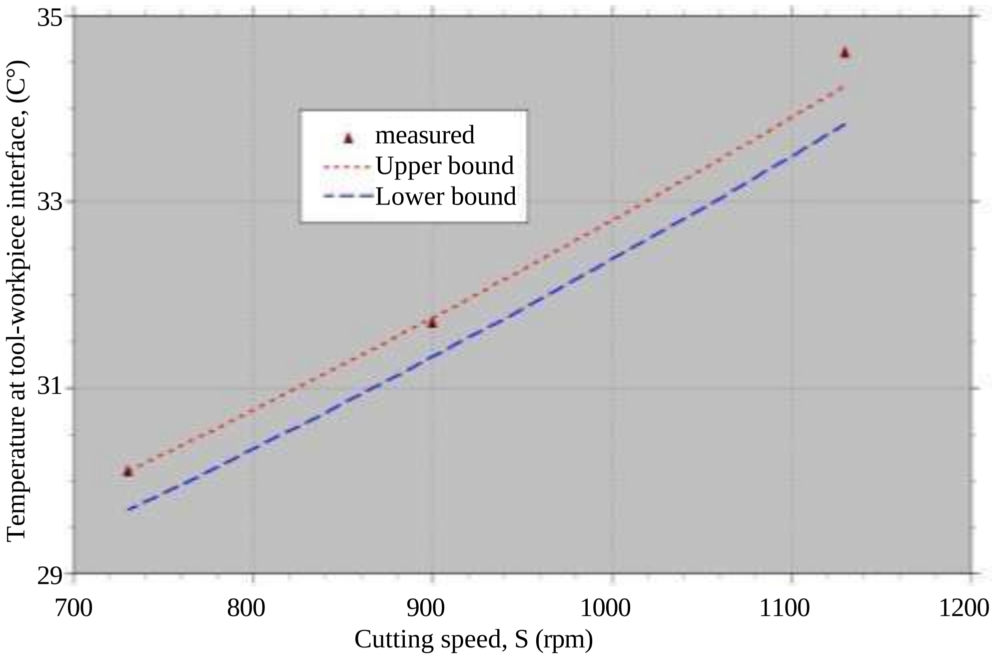

Figure 5. (d) Variation of temperature at the tool-workpiece interface (Temp) with the cutting speed (S) for a given feed rate, F1=400 mm/min and depth-of-cut, DOC1=0.15 mm.

CONCLUDING REMARKS

This paper aims to determine the optimal machining parameters for Al6351 alloy plates, considering four key performance indicators: surface roughness (Ra), material removal rate (MRR), resulting forces (RF), and the temperature at the tool-workpiece interface (Temp). A Taguchi L9OA (orthogonal array) was implemented to analyze the effects of three machining parameters – cutting speed (S), feed rate (F), and depth-of-cut (DOC) – each at three distinct levels.

A modified Taguchi method was used to statistically analyze the experimental data. This analysis resulted in empirical equations linking the machining parameters to the performance characteristics. The validity of these models was confirmed through experimental verification.

These validated equations were then used to predict the range of each performance characteristic based on different machining parameter combinations. Multi-objective optimization was employed to simultaneously minimize Ra, RF, and Temp, while maximizing MRR. The optimal parameter combination was identified as a cutting speed of 1130 rpm, a feed rate of 400 mm/min, and a depth-of-cut of 0.15 mm. All calculations were carried out using Excel.

The performance of the modified Taguchi method was compared against several heuristic optimization algorithms: Harmony Search Algorithm (HSA), Particle Swarm Optimization (PSO), Genetic Algorithm (GA), and Hybrid Artificial Bee Colony (HABC) algorithm. The results indicate that the modified Taguchi method provides significantly better performance for optimizing conventional milling operations.

Future work is directed towards the development and characterization of AA6351 reinforced with Al_2O_3 in different weight proportions using stir casting method.

ACKNOWLEDGMENT

The authors also like to acknowledge the K L University for providing support.

Funding

This research did not receive any specific funding.

Conflicts of Interest

The authors have nothing to disclose.

Data availability statement

All the relevant data are included in the manuscript. No separate repository is attached. There is no additional data available for this study.

Author contribution statement

K. Sri Manikanta: Writing & editing the manuscript. S. Lokesh: Writing – original draft, Formal analysis.

K. Prasanth Kumar Reddy: Writing – review & editing, Writing – original draft, Formal analysis. V. Sai Akshara: Review & editing, Data validation, Boggarapu Nageswara Rao: Writing – review & editing, Data validation, Supervision, Conceptualization, Formal analysis. Muni Tanuja Anantha: Data validation, Supervision.

REFERENCES

1. H. S. Ram, M. Uthayakumar, S. S. Kumar, S. T. Kumaran, B. Azzopardi, and K. Korniejenko, Prediction of Kerf Width and Surface Roughness of Al6351 Based Composite in Wire-Cut Electric Discharge Machining Using Mathematical Modelling, Materials 2022, Vol. 15, Page 1102 15, 1102 (2022).
2. A. A. Premnath, T. Alwarsamy, and T. Rajmohan, Experimental Investigation and Optimization of Process Parameters in Milling of Hybrid Metal Matrix Composites, Materials and Manufacturing Processes 27, 1035 (2012).
3. T. Sathish, N. Sabarirajan, and S. Karthick, Machining parameters optimization of Aluminium Alloy 6063 with reinforcement of SiC composites, Mater Today Proc 33, 2559 (2020).

4. Ö. Seçgin and M. Z. Sogut, Surface roughness optimization in milling operation for aluminum alloy (Al 6061-T6) in aviation manufacturing elements, Aircraft Engineering and Aerospace Technology 93, 1367 (2021).
5. P. Jayaraman, L. Mahesh Kumar, and V. Jayaseelan, Multi-response Optimization of Cutting Parameters During End-milling of AA6101 T6 Aluminium Alloy Using Grey Relational Analysis, International Journal of Applied Engineering Research 10, 4275 (2015).
6. V. V. N. Sarath and N. Tamiloli, Optimization of multiple quality characteristics for end milling under dry cutting environment using desirability function, J Phys Conf Ser 2070, 012218 (2021).
7. R. Sharma, K. Sharma, D. Singh, K. Mausam, and R. P. Singh, Investigation of Optimum Process Parameter on CNC Turning for Aluminium Alloy AA6262 Using Grey Relational Analysis, Lecture Notes in Mechanical Engineering 611 (2021).
8. N. TAMILOLI, J. VENKATESAN, T. KUMAR, A. ASHWIN, and Z. KALITCHIN, MILLING PARAMETERS ON AA-6082-T6 ALLOY USING GRAY RELATIONAL ANALYSIS, REGRESSION, ANN, AND GA MODELS, Journal of the Balkan Tribological Association 28, 233 (2022).
9. M. Manoharan, A. Kulandaivel, A. Arunagiri, M. R. A. Refaai, S. Yishak, and G. Buddharsamy, Statistical Modelling to Study the Implications of Coated Tools for Machining AA 2014 Using Grey Taguchi-Based Response Surface Methodology, Advances in Materials Science and Engineering 2021, 6843276 (2021).
10. Z. Xing, H. Dai, J. Zhang, and Y. Li, Evaluation and Improvement of Greenness for Milling AL6061 Alloy through Life Cycle Assessment and Grey Relational Analysis, Materials 2022, Vol. 15, Page 8231 15, 8231 (2022).
11. J. Unnikrishna Pillai, I. Sanghrajka, M. Shunmugavel, T. Muthuramalingam, M. Goldberg, and G. Littlefair, Optimisation of multiple response characteristics on end milling of aluminium alloy using Taguchi-Grey relational approach, Measurement 124, 291 (2018).
12. S. Li, J. Sui, F. Ding, S. Wu, W. Chen, and C. Wang, Optimization of Milling Aluminum Alloy 6061-T6 using Modified Johnson-Cook Model, Simul Model Pract Theory 111, 102330 (2021).
13. CHEN Liang-ji and WEI Zi-sen, Multi-objective Synchronous Optimization Method for Milling Parameters and Tool Geometric Parameters of 7075-T651 Aluminum Alloy, SURFACE TECHNOLOGY 51, 263 (2022).
14. Ö. Seçgin and M. Z. Sogut, Parametric Optimization of Machining Criteria for Al 6068 Aluminum Alloy using in Manufacturing Process of Aircraft, Journal of Aeronautics, Astronautics and Aviation 53, 289 (2021).
15. M. Ay and A. Etyemez, Optimization of Effects of Cutting Parameters and Cutting Tool Path by using Grey Based Taguchi Method, Acta Phys Pol A 134, 125 (2018).
16. V. H. Nguyen, T. T. Le, and A. T. Nguyen, Optimization of Process Parameter in High-Speed Milling AA6061 Using SVR and NSGA-II, Lecture Notes in Mechanical Engineering 149 (2024).
17. P. P. Das, Application of EDAS method in parametric optimization of vertical milling operation on Al 6063, AIP Conf Proc 2786, (2023).
18. W. H. Wang, X. Cheng, Q. L. Sun, F. Wang, and X. M. Yang, Study on tool wear for mircomilling of 6061 aluminium alloy, IOP Conf Ser Mater Sci Eng 504, 012084 (2019).
19. S. Rajendran and S. C. Rasheedali, Optimization of process parameters for peripheral milling operation using Taguchi grey relational analysis, AIP Conf Proc 2134, (2019).
20. S. S. Warsi, M. H. Agha, R. Ahmad, S. H. I. Jaffery, and M. Khan, Sustainable turning using multi-objective optimization: a study of Al 6061 T6 at high cutting speeds, International Journal of Advanced Manufacturing Technology 100, 843 (2019).
21. S. Tesic, D. Cica, S. Borojevic, B. Sredanovic, M. Zeljkovic, D. Kramar, and F. Pusavec, Optimization and Prediction of Specific Energy Consumption in Ball-End Milling of Ti-6Al-4V Alloy Under MQL and Cryogenic Cooling/Lubrication Conditions, International Journal of Precision Engineering and Manufacturing - Green Technology 9, 1427 (2022).
22. P. HEMA, G. PADMANABHAN, and T. ESWAR, EXPERIMENTAL INVESTIGATION AND OPTIMIZATION OF MACHINING PARAMETERS IN MILLING OF AL6351 USING

HYBRID - ARTIFICIAL BEE COLONY ALGORITHM, I-Manager's Journal on Mechanical Engineering 9, 9 (2019).
23. P. J. Ross, Taguchi Techniques for Quality Engineering., Singapore., https://www.scirp.org/%28S%28vtj3fa45qm1ean45vvffcz55%29%29/reference/referencespapers.aspx?referenceid=1333944.
24. M. T. Anantha, S. Koneru, S. Pyatla, P. P. T. Pillai, T. Buddi, and N. R. Boggarapu, Optimal Constrained Groove Pressing Process Parameters Applying Modified Taguchi Technique and Multi-Objective Optimization, Pertanika J Sci Technol 32, 883 (2024).
25. G. Satyanarayana, K. L. Narayana, and B. Nageswara Rao, Identification of Optimum Laser Beam Welding Process Parameters for E110 Zirconium Alloy Butt Joint Based on Taguchi-CFD Simulations, Lasers in Manufacturing and Materials Processing 5, 182 (2018).
26. B. V. Dharmendra, S. P. Kodali, and B. Nageswara Rao, A simple and reliable Taguchi approach for multi-objective optimization to identify optimal process parameters in nano-powder-mixed electrical discharge machining of INCONEL800 with copper electrode, Heliyon 5, (2019).
27. S. Koneru, A. Srinath, and B. Nageswara Rao, Multiobjective optimization for the optimal heat pipe working parameters based on Taguchi's design of experiments, Heat Transfer 51, 2510 (2022).
28. M. T. Anantha, T. Buddi, and N. R. Boggarapu, Multi-objective optimization basing modified Taguchi method to arrive the optimal die design for CGP of AZ31 magnesium alloy, International Journal on Interactive Design and Manufacturing 18, 6451 (2023).
29. A. M. Tanuja, H. Mugutkar, S. Pyatla, K. P. K. Reddy, and B. N. Rao, Multi- Objective Optimization to Specify Optimal Friction Stir Welding Process Parameters for Dissimilar Mg Alloys (AZ31 and ZM21), International Journal of Vehicle Structures and Systems 16, 50 (2024).
30. M. T. Anantha, S. Koneru, P. P. Thiruvambalam Pillai, N. R. Boggarapu, T. Buddi, K. I. Usanova, and R. Deorari, Surface quality improvement of AZ31 Mg alloy by a combination of modified Taguchi method and simple multi objective optimization procedure, Cogent Eng 11, (2024).
31. K. P. Kumar Reddy, S. R. Kumar, and B. Nageswara Rao, Multi-objective optimization for minimize cutting force and power consumption in corn stalk chopping processes, Heliyon 10, (2024).
32. K. P. K. Reddy, B. N. Rao, M. N. Nazeemudheen, S. K. Manwatkar, and S. V. S. N. Murty, Selection of Optimal Process Parameters to Obtain Defect-Free Builds in IN718 Made by Laser Powder Bed Fusion, J Mater Eng Perform 33, 10228 (2023).
33. R.K. Prasanth Kumar, N. R. Boggarapu, and S. V. S. Narayana Murty, Multi- objective optimization to specify optimal selective laser melting process parameters for SS316 L powder, Multidiscipline Modeling in Materials and Structures 20, 59 (2023).